Detection of synchronous brain activity in white matter tracts at rest and under functional loading

Zhaohua Ding[a,b,c,1], Yali Huang[a,d], Stephen K. Bailey[e], Yurui Gao[a,c], Laurie E. Cutting[e,f,g], Baxter P. Rogers[a,h], Allen T. Newton[a,h], and John C. Gore[a,c,e,f,h]

[a]Vanderbilt University Institute of Imaging Science, Vanderbilt University, Nashville, TN 37232; [b]Department of Electrical Engineering and Computer Science, Vanderbilt University, Nashville, TN 37232; [c]Department of Biomedical Engineering, Vanderbilt University, Nashville, TN 37232; [d]College of Electronics and Information Engineering, Hebei University, Baoding 071002, People's Republic of China; [e]Vanderbilt Brain Institute, Vanderbilt University, Nashville, TN 37232; [f]Vanderbilt Kennedy Center, Vanderbilt University, Nashville, TN 37232; [g]Peabody College of Education and Human Development, Vanderbilt University, Nashville, TN 37232; and [h]Department of Radiology and Radiological Sciences, Vanderbilt University Medical Center, Nashville, TN 37232

Edited by Marcus E. Raichle, Washington University in St. Louis, St. Louis, MO, and approved December 5, 2017 (received for review June 28, 2017)

Functional MRI based on blood oxygenation level-dependent (BOLD) contrast is well established as a neuroimaging technique for detecting neural activity in the cortex of the human brain. While detection and characterization of BOLD signals, as well as their electrophysiological and hemodynamic/metabolic origins, have been extensively studied in gray matter (GM), the detection and interpretation of BOLD signals in white matter (WM) remain controversial. We have previously observed that BOLD signals in a resting state reveal structure-specific anisotropic temporal correlations in WM and that external stimuli alter these correlations and permit visualization of task-specific fiber pathways, suggesting variations in WM BOLD signals are related to neural activity. In this study, we provide further strong evidence that BOLD signals in WM reflect neural activities both in a resting state and under functional loading. We demonstrate that BOLD signal waveforms in stimulus-relevant WM pathways are synchronous with the applied stimuli but with various degrees of time delay and that signals in WM pathways exhibit clear task specificity. Furthermore, resting-state signal fluctuations in WM tracts show significant correlations with specific parcellated GM volumes. These observations support the notion that neural activities are encoded in WM circuits similarly to cortical responses.

fMRI | BOLD | functional connectivity | functional activity | white matter

Blood oxygenation level-dependent (BOLD) contrast has for several years been the established basis for detecting localized neural activity in the human brain using functional magnetic resonance imaging (fMRI) (1, 2). While BOLD signals have been robustly detected in brain gray matter (GM) in a large number of studies, whether such signals reliably arise in white matter (WM) remains controversial (3). Fundamentally, the biophysical origins of BOLD signals in WM are not clear, along with whether neural signaling in WM triggers changes in BOLD signals similar to GM. Heeger and Ress (4) demonstrated that BOLD signals are correlated mostly with postsynaptic spiking activity, supporting the idea that neural events within WM may also produce BOLD signals. However, Logothetis et al. (5) observed that BOLD signals from cortex are primarily correlated with local field potentials (LFPs), and the equivalent processes are not obvious in WM. Mukamel et al. (6) found that BOLD signals are correlated with both postsynaptic spiking activity and LFPs, thus harmonizing these dichotomous arguments. Moreover, it is clear that BOLD effects are robustly detectable in WM following vasodilation from hypercapnia and vary with different levels of neural activity induced by anesthesia (7, 8). Whether BOLD changes couple directly to changes in WM activity within tracts is unclear.

There thus remains a need for clear evidence that BOLD effects in WM are directly related to neural activity. However, reports of successful demonstrations to date are quite sparse. This may be partly attributable to the much reduced vascular density in WM (9), so that much lower BOLD signal changes are expected. However, despite the large differences in vascular density between GM and WM, the oxygen extraction fraction has been shown to be relatively uniform throughout the parenchyma of a resting brain (10). In addition, cerebral blood flow-normalized BOLD signal changes in response to hypercapnia are found to be largely comparable in WM and GM (7). Furthermore, it has been observed that BOLD signals in a resting state exhibit similar temporal and spectral profiles in both GM and WM of the human brain (11) and that their relative low-frequency (0.01–0.08 Hz) signal powers are comparable (12). These findings together suggest that BOLD signals in WM may also reflect neural activity and may be detectable using appropriately sensitive imaging and analysis techniques.

By using appropriate techniques that take into account the unique characteristics of BOLD signals in WM, a number of studies have reported reliable observations of WM activations (13). For instance, Mazerolle et al. (14) detected robust BOLD activations in the posterior limb of internal capsule imaged with a high field of 4 T; and by incorporating 4-T imaging with an asymmetric spin echo spiral sequence, Gawryluk et al. (15) observed BOLD signals in the anterior corpus callosum. Detection of BOLD signals in WM has also been enhanced by using specialized task paradigms (16) or improved data analysis methods (17).

We have previously observed that BOLD signals in a resting state exhibit structure-specific anisotropic temporal correlations in WM (11, 12). On the basis of these findings, we proposed a concept of spatiotemporal correlation tensors that characterize correlational anisotropy in WM BOLD signals. We found that, along many WM tracts, the directional preferences of spatiotemporal correlation tensors in a resting state are grossly consistent with those revealed by diffusion tensors and that external

Significance

Functional MRI has been widely used to assess the functional architecture of the brain based on detecting changes in neural activity in gray matter via blood oxygenation level-dependent (BOLD) effects. However, the existence and possible relevance of BOLD signals in white matter remain controversial. We demonstrate that BOLD signals in functional cortical volumes are strongly correlated with signals in specific, segmented white matter tracts in a resting state, and the correlations can be modulated by specific functional loadings. We therefore show that current concepts of functional connectivity based on synchronous BOLD correlations may be extended to include white matter and that changes in neural activity are encoded in BOLD variations throughout the brain.

Author contributions: Z.D., L.E.C., and J.C.G. designed research; Z.D., Y.H., and S.K.B. performed research; Y.H., Y.G., B.P.R., and A.T.N. analyzed data; and Z.D. wrote the paper.

The authors declare no conflict of interest.

This article is a PNAS Direct Submission.

[1]To whom correspondence should be addressed. Email: zhaohua.ding@vanderbilt.edu.

This article contains supporting information online at www.pnas.org/lookup/suppl/doi:10.1073/pnas.1711567115/-/DCSupplemental.

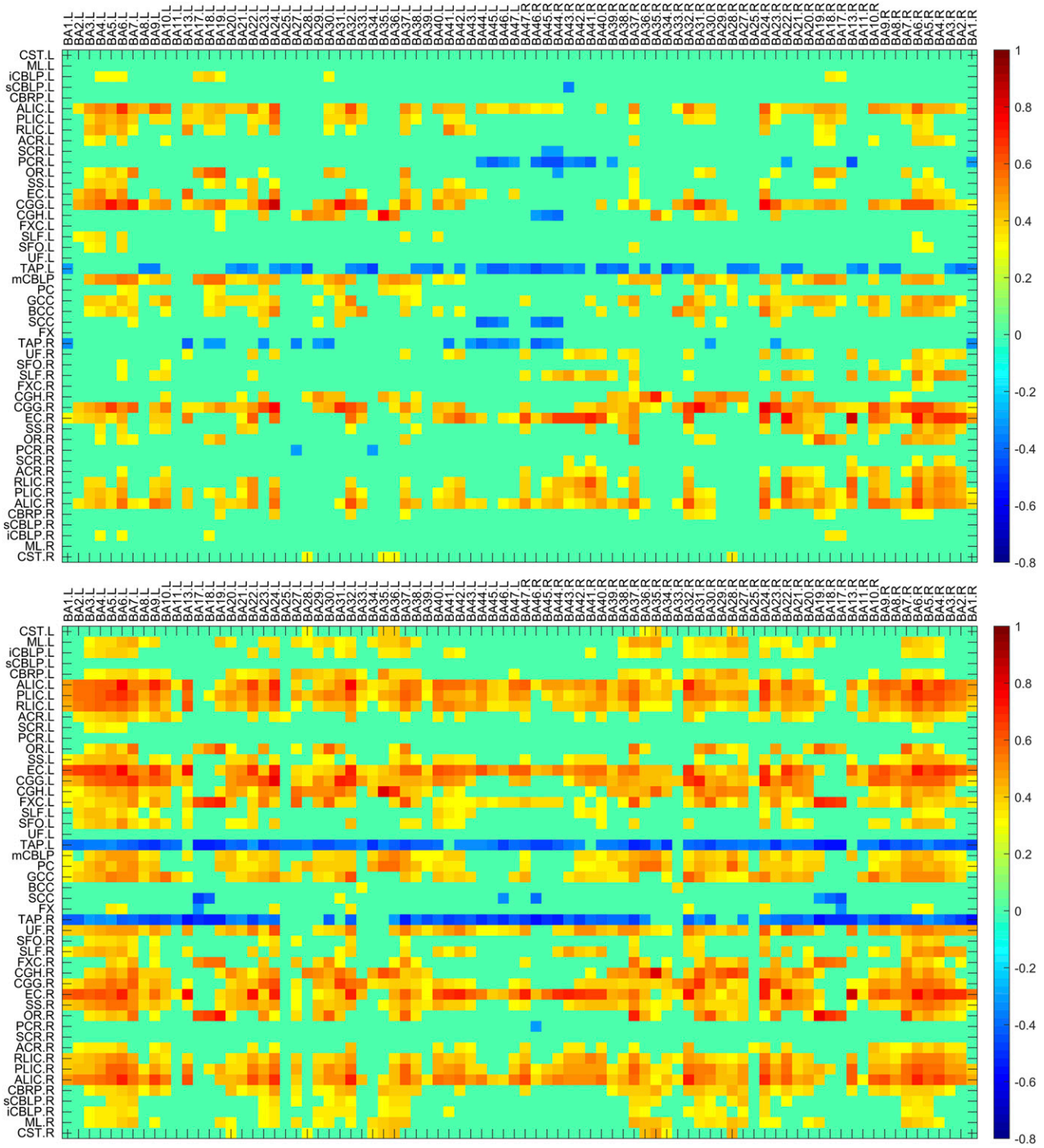

Fig. 1. Maps of temporal correlations between BOLD signals in WM bundles and GM regions. *Top* and *Bottom* panels are for resting state and visual stimulation, respectively, with each averaged over 12 subjects studied and thresholded at mean $|CC| > 0.3$. Stimulation-induced increases in temporal correlations between WM and GM regions are seen as darker colors. The horizontal stripes suggest the existence of synchronicity between segmented WM and GM volumes, which is enhanced by visual stimulation. BA denotes Brodmann area, and abbreviations for WM bundles are listed in *Supporting Information*.

stimuli tend to enhance visualization of relevant fiber pathways. These findings support the concept that variations in WM BOLD signals are related to tract-specific neural activity. We have more recently shown that sensory stimulations induce explicit BOLD responses along parts of the projection fiber pathways (18). The purpose of this study is to demonstrate more comprehensively that BOLD signals in WM reflect specific neural activities both in resting state and in stimulus-evoked conditions. We show that resting-state fMRI signal correlations are detectable between WM tracts and specific GM functional areas and that these can be modulated by functional loading. Furthermore, we confirm that BOLD signals in relevant WM pathways are modulated

synchronously with the time course of a stimulus and that such activated WM pathways exhibit high specificity to functional loading. All of these findings converge to support the notion that neural activities are embedded in WM BOLD signals and that these reveal specific neural connections.

Results

Resting-State Correlations Between WM and GM in the Human Brain. The average temporal correlations in a resting state between BOLD signals in 48 WM bundles and 84 GM regions are shown in Fig. 1, *Top*, in which each element is the correlation coefficient (CC) between a pair of WM and GM regions averaged across 12 subjects studied. It is quite apparent that the CC variations are not random, but rather manifest as patterns of horizontal stripes, suggesting that certain WM bundles exhibit overall greater temporal correlations with GM. Mean CC of the WM bundles across the GM regions are given in Fig. 2 (red bars), which shows that bilateral anterior limb of internal capsule (ALIC) and cingulum (gyrus) (CGG), middle cerebellar peduncle (CBLP), genu of corpus callosum (GCC), right external capsules (EC), and posterior limb of internal capsules (PLIC), had greater mean CC (>0.3) than other WM bundles. There were also negative correlations between some of the WM bundles and GM regions. Most notably, the left tapetum (TAP) had quite pronounced negative correlations with most of the GM regions (mean CC < −0.3). The patterns of horizontal stripes tend to suggest the existence of synchronous activities within segmented WM and GM volumes in the human brain, which suggest there are specific patterns of connections during resting-state brain activity.

Mean power spectra of WM and GM regions over the 12 subjects studied are shown in Fig. S1. It can be observed that both WM and GM regions tend to have increased power toward lower frequencies, although WM has smaller power than GM below 0.05 Hz. Fractional amplitude of low-frequency fluctuations (fALFF) are shown in Fig. S2*A* for the 48 WM bundles. Compared with the mean fALFF of randomly permuted individual BOLD time series (Fig. S2*B*), the mean fALFF in WM is ∼9% greater while the mean fALFF in GM is ∼12% greater. Bootstrap analysis shows that the fALFF is positively correlated with the *Z* score of the mean CC (Fig. S3, blue curve).

Enhancement of Synchronicity Between WM and GM by Functional Loading. Temporal correlations between BOLD signals in the WM bundles and GM regions under visual stimulation are shown in Fig. 1, *Bottom*. It can be readily appreciated that, overall, visual stimulations increased the temporal correlations between the WM and GM regions. Quantitative comparisons in GM-averaged CC of each bundle with the resting state are given in Fig. 2, which shows that 27 WM bundles had significantly increased mean CC ($P < 0.05$, paired and two-tailed *t* tests, uncorrected); two-thirds of these bundles had mean CC above 0.3 under visual stimulation, which included bilateral ALIC and PLIC, bilateral retrolenticular part of IC (RLIC), bilateral EC, bilateral fornix (cres) (FXC), bilateral cingulum (hippocampus) (CGH), left medial lemniscus (ML), right sagittal stratum (SS), right optic radiation (OR), pontine crossing (PC), right uncinate fasciculus (UF), and right cerebral peduncle (CBRP).

Activation of WM by Functional Loading. For all of the WM bundles, the power spectra of mean BOLD signals across the 12 subjects under visual stimulation were derived by Fourier transform, and the values corresponding to the stimulus frequency (∼0.017 Hz) are shown in Fig. 3. Different WM bundles were found to exhibit different signal powers, among which OR, FXC, and splenium of corpus callosum (SCC) had the largest values, followed by PC, TAP, and ML. The anatomical locations of these WM bundles are shown in Fig. S4*A*, in which the bundles are superimposed onto T_1-weighted images.

The magnitudes of the modulations in the BOLD signals from these WM bundles averaged over the 12 subjects studied are depicted in Fig. 4, along with the waveform of the stimulus and average signal variation in the primary visual cortex (V1, BA17). The power spectra of these waveforms are provided at the bottom of each signal wave. Evidently, signals from these bundles exhibited clear periodicity related to the stimulus, which was reflected in the power spectra as well by the coincidences of their peaks with those of the stimulus. It can also be seen that these WM bundles exhibited different time delays (TDs) relative to the stimulus. In particular, the waveforms of the SCC and bilateral TAP signals were ∼180° out of phase relative to the stimulus, which could largely account for the negative correlations observed in Fig. 1. The TD values for each of these WM bundles were quantified by first averaging the waveforms across the seven stimulus periods. The time point of maximum cross-correlation between the averaged waveforms and the stimulus convolved with the canonical hemodynamic response function (HRF) was then selected. Fig. S5*A* shows the original stimulus waveform before and after convolution with the HRF, and the average signal waveforms in V1 and in each of the WM bundles. Consistent with the observations in Fig. 4, seven WM bundles had small TDs (right OR, 1.6 s; left OR, 4.4 s; right FXC, 0 s; left FXC, 0 s; PC, 8.2 s; right ML, 5.6 s; left ML, 5.2 s), while SCC and TAP had a TD of nearly half a stimulus cycle (SCC, 27.6 s; right TAP, 29.2 s; and left TAP, 33.4 s).

Correlations between these WM bundles and mean signal from the visual cortices (V1–V5, BA17–19) during resting state and visual stimulations are summarized in Table S1. Note that except for the left OR, for which the correlation was high during a resting state, the other nine bundles exhibited increased correlations

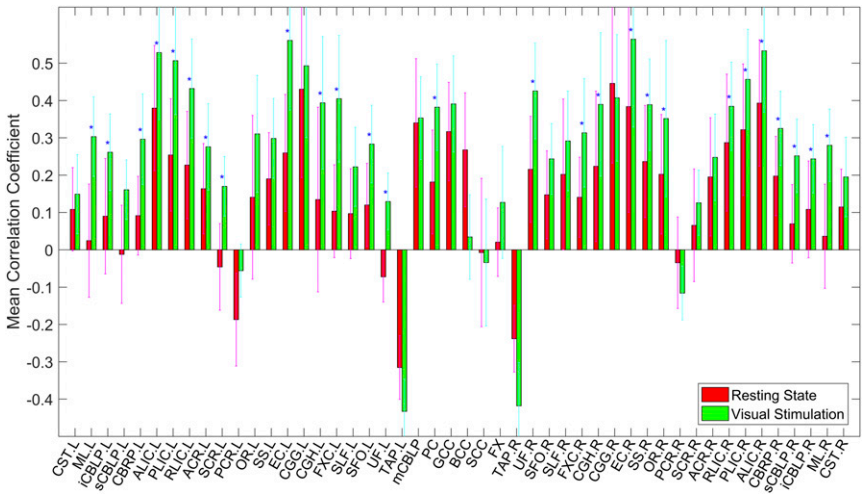

Fig. 2. GM-averaged correlation coefficients of WM bundles in a resting state (red) and under visual stimulation (green). Mean and SD are shown, and blue stars (*) denote $P < 0.05$ from paired and two-tailed *t* tests of *Z* score of the mean CC.

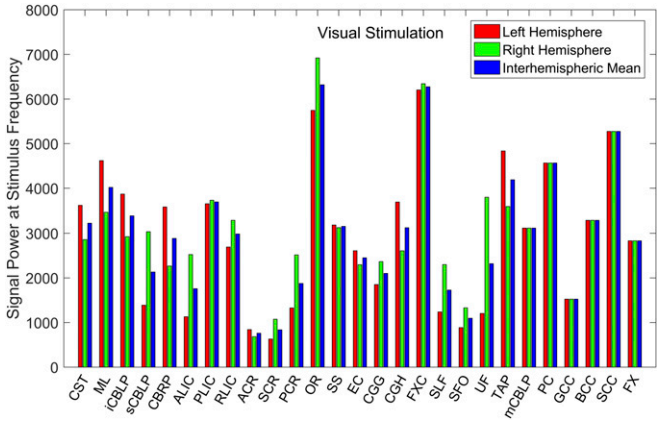

Fig. 3. Power of mean BOLD signals in WM bundles at stimulus frequency during visual stimulation. The interhemispheric means of OR, FXC, TAP, and ML and signal power of SCC and PC are above 4,000, which is one-half of the mean signal power in the primary visual cortex.

under visual stimulations and six of the increases were significant ($P < 0.05$, uncorrected). The three bundles (PC and bilateral ML) not showing significant changes are located in the brainstem and cerebellum; they are likely related to eye movement or sensory processing and thus not directly involved in visual perception.

Task Specificity of WM Activations to Functional Loading. Powers of mean BOLD signals in the WM bundles at the stimulus frequency under sensory stimulations and motor tasks are shown in Fig. 5. With right-hand stimulation, the WM bundles exhibiting strong BOLD signal variations were bilateral corticospinal tract (CST), bilateral ML, right inferior and superior CBLP, bilateral CBRP, left ALIC, bilateral CGG and CGH, and PC; with left-hand stimulation, the WM bundles exhibiting strongest power of BOLD signals were bilateral CST, bilateral ML, bilateral inferior and superior CBLP, bilateral CBRP, bilateral ALIC and PLIC, left RLIC, left SS, bilateral CGG and CGH, right UF, middle CBLP and PC. The responses to sensory stimulation were widespread, but most were within the sensorimotor circuits. Of particular note, while the function of UF is not known yet, the CGG and CGH are connected to the posterior cingulate cortex, which has been confirmed to be responsive to somatosensory stimulation (19). Responses to the motor tasks were less pronounced, with only right ALIC and left PLIC strongly responsive to right-hand motor task and left inferior CBLP, bilateral CBRP, left PLIC, and middle CBLP to the left-hand motor task (see Fig. S4 for anatomical locations of these WM bundles).

Differences in WM responses to functional tasks were tested with ANOVA (Table S2). As can be seen, eight WM bundles exhibited significant differences in task responses ($P < 0.05$, uncorrected): bilateral OR, right CGH, bilateral FXC, left superior fronto-occipital fasciculus (SFO), PC, and the body of corpus callosum (BCC).

Analysis of Potential Confounds. Correlations of the measured signal-to-noise ratio (SNR) of WM bundles with the Z score of the mean CC and fALFF using bootstrap analysis were 0.01 and 0.07, respectively, as shown in Fig. S3 (red and green curves), which were much smaller than the correlation of 0.34 between fALFF and the Z score. This indicates that the specific patterns of WM correlations were primarily driven by low-frequency BOLD fluctuations rather than SNR differences between these WM bundles.

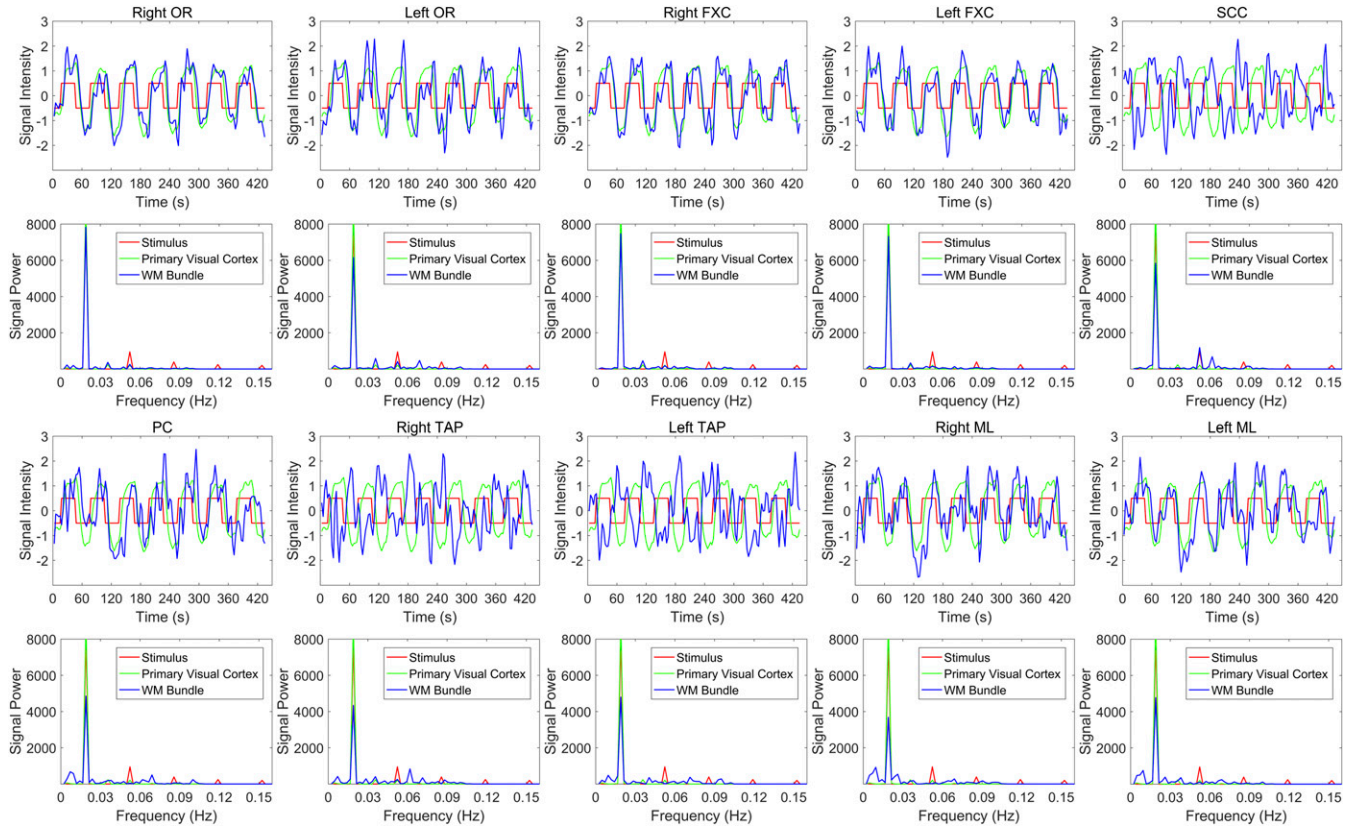

Fig. 4. Signal waveforms and their power spectra in the WM bundles exhibiting greatest signal power at the stimulus frequency. Red, green, and blue curves are the stimulus waveform, the signal in primary visual cortex, and the signal in WM bundles, respectively, along with their corresponding power spectra in the *Bottom*. The signal waveforms are averaged across the 12 subjects studied and exhibit periodic variations with time.

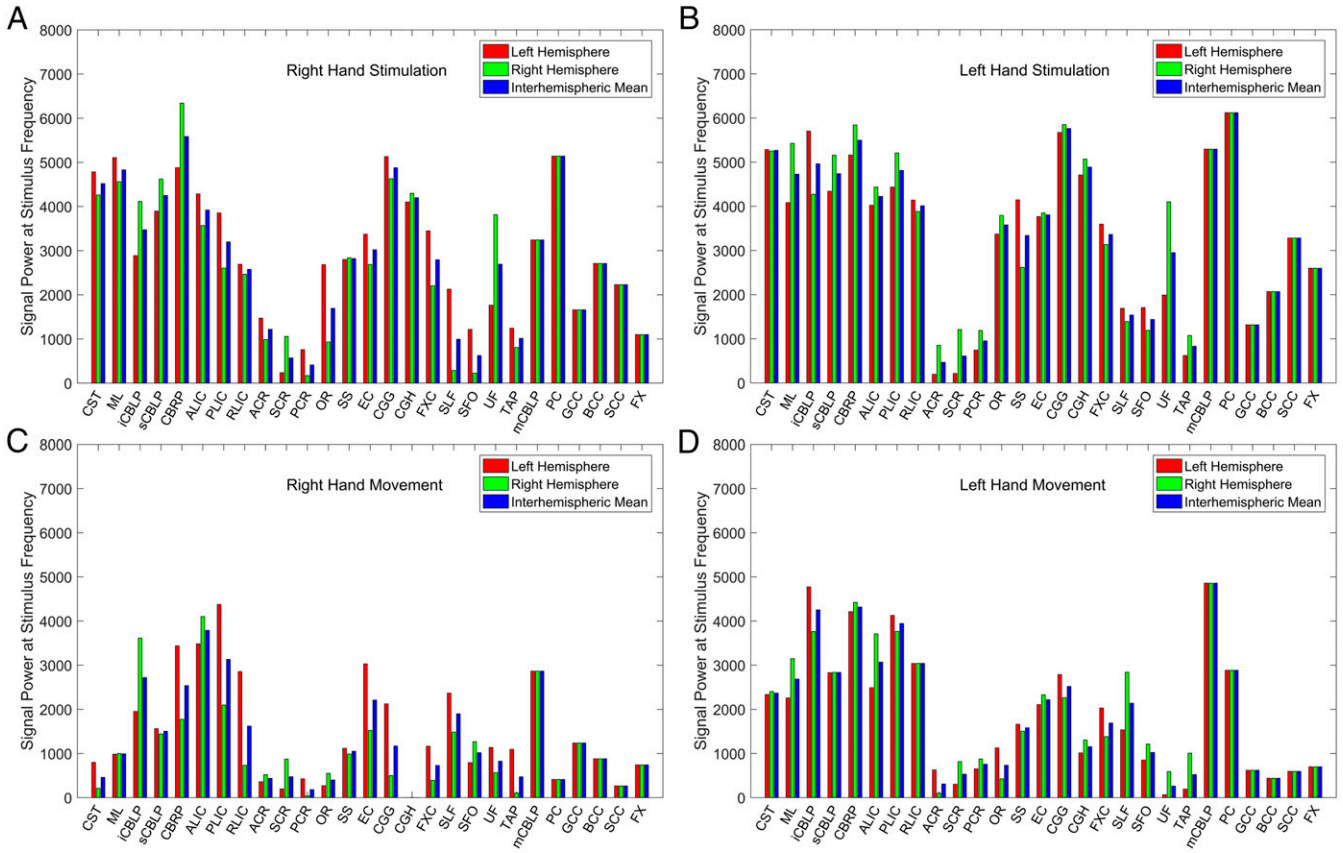

Fig. 5. Power of mean BOLD signals in WM bundles at stimulus frequency during sensory stimulations and motor tasks. Left (*A* and *C*) and right (*B* and *D*) columns are for right and left hands, respectively, and top (*A* and *B*) and bottom (*C* and *D*) rows are for sensory stimulations and motor tasks respectively. The WM bundles exhibiting strong power in response to sensory stimulations and motor tasks are different from those under visual stimulation in Fig. 3, and overall, sensory stimulations particularly to the left hand evoke stronger responses in WM than the motor tasks.

The correlation map computed from mismatched WM–GM pairs is shown in Fig. S6. As expected, the map has nearly zero mean, with maximum CC < 0.15. Resting-state signals and random permutations of BOLD time series acquired with functional tasks had considerably smaller power spectra at the stimulus frequency than the task power in Figs. 3 and 5 (Fig. S7). The results from these analyses suggest that the patterns we observed were not artificially caused by inherent BOLD propagation patterns or processing procedures.

Signal profiles of the WM tract skeletons and their expansions of the WM bundles exhibiting strong power responses to visual stimulations are shown in Fig. S5 *C*–*F*. It can be seen that the skeleton and each of the three expansions had nearly identical signal profiles to those of the original WM in Fig. S5*A*, all of which appeared to be quite different from the waveform in the visual cortex. This indicates that our observations were not due to spreading effects from nearby structures (*Discussion*).

Discussion

General Findings. We observed strong correlation patterns that suggest there is synchronous neural activity within specific cortical volumes and specific WM tracts in the human brain that are detectable by fMRI in a resting state and that can be enhanced by functional loading. These specific patterns suggest a sharing of functional roles between WM and GM directly via structural connections or indirectly through associated regions. The BOLD responses to visual stimulation in those WM bundles that are affected strongly exhibit widely variable TDs. Different stimulations or tasks elicit responses in different and specific groups of WM bundles. Together, these findings support the notion that BOLD signals in WM encode neural activities as well.

Visual Experiments. Under visual stimulation, 10 WM bundles revealed strong synchronous responses to the stimuli, and these included bilateral OR and FXC, SCC, PC, and bilateral TAP and ML. The OR connects the lateral geniculate nuclei of the thalamus to V1, which serves to transmit neural activity to the visual area (20). The function of the fornix has not been completely determined, but there have been some reports of its association with visual memory (21, 22). The SCC contains WM tracts that join the visual cortices of the two hemispheres, and has been implicated in coordinating interhemispherical visual activities (23, 24). WM tracts in the PC carry neural signals from the thalamus to the cerebellum and medulla through the pons, and are functionally related to eye movements (25). While reports on the function of the TAP are rare, this structure has been shown to degenerate together with the OR in subjects with visual deficits (26), suggesting its role in visual processing. The ML conveys sensory neural signals from the face and eyes to the thalamus (27), and thus presumably has relevance to visual responses.

These WM bundles were also found to respond to visual stimulation with different TDs as judged from the phase of each signal waveform. At one extreme, the FXC and the OR had only a brief TD; on the other extreme, the SCC and TAP had TDs of about half a cycle of the stimuli. It seems unlikely that the long TDs were caused by different hemodynamic responses in these bundles (28); but rather, it is more likely that the delays indicate these bundles mediate an inhibitory or deactivating function (24).

Task Specificity of WM Signals. The specificity of WM signals to functional loading was demonstrated by experiments comparing responses to sensory and motor stimuli. In contrast to visual stimulations, the WM bundles that showed strong responses to

sensory and motor activity were primarily parts of, or associated with, the known sensorimotor pathways of established functional neuroanatomy; and compared with the right hand, WM BOLD responses tended to be stronger for left-hand stimulations and tasks. Previously, it was reported that it takes greater efforts for the nonpreferred hand to perform the same task than the preferred hand (29). This is in keeping well with our findings since all of the subjects in this study are right-handed. It was also documented that right-handed males have less pain sensitivity in the preferred hand than the nonpreferred hand (30). Thus, it is reasonable that the left hand is more sensitive to tactile stimulations as well and elicits stronger neural activity in the brain when stimulated.

It should be noted that increased activity in WM is necessarily accompanied by increases in its metabolic demands. Although this work did not examine the metabolism, a recent study found evidence of different metabolic rates in WM under different functional states (31), which is similar to GM. The findings from our study, along with that in ref. 31, suggest that regressing out WM signals should be cautious since these signals also encode neural activities (32, 33).

Limitations. A limitation of this study is that the time series was sampled at relatively low temporal resolution of 3 s, which was interpolated to 0.2 s for computing TDs in WM signals. A similar interpolation approach was adopted by Mitra et al. (34), who derived a highly reproducible TD of the order of 1 s. Nonetheless, we recognize that the temporal resolution of our data acquisition, as well as the quantification method used, may impose some upper bound on the accuracy of the TDs computed, and thus caution that the reported TDs not be overinterpreted.

Another potential limitation is the effect of partial volume averaging. A widely held concern on WM BOLD studies is that the reported activations are due to the confounding effects from adjacent GM and vasculature. We have been fully aware of this potential confound and have tried to meticulously address it in our earlier studies (8, 12). In this work, to avoid potential influences from adjacent structures, we used a WM mask that was tightly thresholded (>0.95). Our further experiments with visual stimulations demonstrate that the signal profiles of WM bundles of various thickness were highly comparable and that the waveform in the SCC was ∼180° out of phase with GM, indicating that the partial volume effect was quite minimal if it existed.

In conclusion, this study demonstrates that BOLD signals in specific WM tracts exhibit patterns of correlations to specific cortical volumes and that the waveforms in stimulus-relevant WM pathways are synchronous with the applied stimuli but with various degrees of TD. Signals in WM pathways exhibit clear task specificity. Our statistical analysis shows that these observations were not driven by artifacts from the imaging or processing procedures, and the correlation of WM-GM is positively correlated with fALFF. These findings provide strong evidence that BOLD signals in WM reflect neural activities both in a resting state and under functional loading.

Methods

Full-brain MRI data were acquired from 16 healthy and right-handed adult volunteers (eight males; age, 28.1 ± 4.6 y). No subjects had a history of neurological, psychiatric, or medical conditions as determined by interview. Before imaging, each subject gave informed consent according to protocols approved by the Vanderbilt University Institutional Review Board. Detailed image acquisition, processing, and analysis procedures are provided in *Supporting Information*.

ACKNOWLEDGMENTS. This work was supported by NIH Grants R01 NS093669 (to J.C.G.), R01 HD044073 (to L.E.C.), R01 HD067254 (to L.E.C.), U54 HD083211 (to L.E.C.), and F31 HD090923 (to S.K.B.).

1. Ogawa S, Lee TM, Kay AR, Tank DW (1990) Brain magnetic resonance imaging with contrast dependent on blood oxygenation. *Proc Natl Acad Sci USA* 87:9868–9872.
2. Fox MD, Raichle ME (2007) Spontaneous fluctuations in brain activity observed with functional magnetic resonance imaging. *Nat Rev Neurosci* 8:700–711.
3. Logothetis NK, Wandell BA (2004) Interpreting the BOLD signal. *Annu Rev Physiol* 66: 735–769.
4. Heeger DJ, Ress D (2002) What does fMRI tell us about neuronal activity? *Nat Rev Neurosci* 3:142–151.
5. Logothetis NK, Pauls J, Augath M, Trinath T, Oeltermann A (2001) Neurophysiological investigation of the basis of the fMRI signal. *Nature* 412:150–157.
6. Mukamel R, et al. (2005) Coupling between neuronal firing, field potentials, and FMRI in human auditory cortex. *Science* 309:951–954.
7. Rostrup E, et al. (2000) Regional differences in the CBF and BOLD responses to hypercapnia: A combined PET and fMRI study. *Neuroimage* 11:87–97.
8. Wu TL, et al. (2016) Effects of anesthesia on resting state BOLD signals in white matter of non-human primates. *Magn Reson Imaging* 34:1235–1241.
9. Nonaka H, et al. (2003) Microvasculature of the human cerebral white matter: Arteries of the deep white matter. *Neuropathology* 23:111–118.
10. Raichle ME, et al. (2001) A default mode of brain function. *Proc Natl Acad Sci USA* 98: 676–682.
11. Ding Z, et al. (2013) Spatio-temporal correlation tensors reveal functional structure in human brain. *PLoS One* 8:e82107.
12. Ding Z, et al. (2016) Visualizing functional pathways in the human brain using correlation tensors and magnetic resonance imaging. *Magn Reson Imaging* 34:8–17.
13. Gawryluk JR, Mazerolle EL, D'Arcy RC (2014) Does functional MRI detect activation in white matter? A review of emerging evidence, issues, and future directions. *Front Neurosci* 8:239.
14. Mazerolle EL, et al. (2013) Sensitivity to white matter FMRI activation increases with field strength. *PLoS One* 8:e58130.
15. Gawryluk JR, Brewer KD, Beyea SD, D'Arcy RC (2009) Optimizing the detection of white matter fMRI using asymmetric spin echo spiral. *Neuroimage* 45:83–88.
16. Tettamanti M, et al. (2002) Interhemispheric transmission of visuomotor information in humans: fMRI evidence. *J Neurophysiol* 88:1051–1058.
17. D'Arcy RC, Hamilton A, Jarmasz M, Sullivan S, Stroink G (2006) Exploratory data analysis reveals visuovisual interhemispheric transfer in functional magnetic resonance imaging. *Magn Reson Med* 55:952–958.
18. Wu X, et al. (2017) Functional connectivity and activity of white matter in somatosensory pathways under tactile stimulations. *Neuroimage* 152:371–380.
19. Olson CR, Musil SY (1992) Posterior cingulate cortex: Sensory and oculomotor properties of single neurons in behaving cat. *Cereb Cortex* 2:485–502.
20. Clatworthy PL, et al. (2010) Probabilistic tractography of the optic radiations–An automated method and anatomical validation. *Neuroimage* 49:2001–2012.
21. Botez-Marquard T, Botez MI (1992) Visual memory deficits after damage to the anterior commissure and right fornix. *Arch Neurol* 49:321–324.
22. Miller JP, et al. (2015) Visual-spatial memory may be enhanced with theta burst deep brain stimulation of the fornix: A preliminary investigation with four cases. *Brain* 138: 1833–1842.
23. Saenz M, Fine I (2010) Topographic organization of V1 projections through the corpus callosum in humans. *Neuroimage* 52:1224–1229.
24. Knyazeva MG (2013) Splenium of corpus callosum: Patterns of interhemispheric interaction in children and adults. *Neural Plast* 2013:639430.
25. Bender MB (1980) Brain control of conjugate horizontal and vertical eye movements: A survey of the structural and functional correlates. *Brain* 103:23–69.
26. Gibson JL (1901) Hemianopsia, with reference to the localisation of cerebral diseases. *Australas Med Gaz* 20:271–277.
27. Rainey WT, Jones EG (1983) Spatial distribution of individual medial lemniscal axons in the thalamic ventrobasal complex of the cat. *Exp Brain Res* 49:229–246.
28. Handwerker DA, Ollinger JM, D'Esposito M (2004) Variation of BOLD hemodynamic responses across subjects and brain regions and their effects on statistical analyses. *Neuroimage* 21:1639–1651.
29. Jäncke L, et al. (1998) Differential magnetic resonance signal change in human sensorimotor cortex to finger movements of different rate of the dominant and subdominant hand. *Brain Res Cogn Brain Res* 6:279–284.
30. Pud D, Golan Y, Pesta R (2009) Hand dominancy—a feature affecting sensitivity to pain. *Neurosci Lett* 467:237–240.
31. Thompson GJ, et al. (2016) The whole-brain "global" signal from resting state fMRI as a potential biomarker of quantitative state changes in glucose metabolism. *Brain Connect* 6:435–447.
32. Vos de Wael R, Hyder F, Thompson GJ (2017) Effects of tissue-specific fMRI signal regression on resting-state functional connectivity. *Brain Connect* 7:482–490.
33. Hahamy A, et al. (2014) Save the global: Global signal connectivity as a tool for studying clinical populations with functional magnetic resonance imaging. *Brain Connect* 4:395–403.
34. Mitra A, Snyder AZ, Blazey T, Raichle ME (2015) Lag threads organize the brain's intrinsic activity. *Proc Natl Acad Sci USA* 112:E2235–E2244.
35. Maldjian JA, Laurienti PJ, Kraft RA, Burdette JH (2003) An automated method for neuroanatomic and cytoarchitectonic atlas-based interrogation of fMRI data sets. *Neuroimage* 19:1233–1239.
36. Mori S, et al. (2008) Stereotaxic white matter atlas based on diffusion tensor imaging in an ICBM template. *Neuroimage* 40:570–582.
37. Bürgel U, et al. (2006) White matter fiber tracts of the human brain: Three-dimensional mapping at microscopic resolution, topography and intersubject variability. *Neuroimage* 29:1092–1105.
38. Marussich L, Lu KH, Wen H, Liu Z (2017) Mapping white-matter functional organization at rest and during naturalistic visual perception. *Neuroimage* 146:1128–1141.
39. Zuo XN, et al. (2010) The oscillating brain: Complex and reliable. *Neuroimage* 49: 1432–1445.